Jordanian Journal of Engineering and Chemical Industries

Print ISSN: 2616 - 9584 Online ISSN: 2617 - 720X

Methane Dissociation Over the Rh-Decorated Ni(100) Surface: A Density Functional Theory Investigation

Ibrahim Suleiman[*1)], Niveen Assaf[2)], Michael Stockenhuber[3)], Eric M Kennedy[3)]

[1)]Al Balqa Applied University, Faculty of Engineering Technology, Chemical Engineering Department, Amman 11134, Jordan.
[2)]Al Balqa Applied University, Faculty of Engineering Technology, Chemical Engineering Department, Al-Salt 19117, Jordan.
[3)]The University of Newcastle, School of Engineering, Callaghan, NSW 2308, Australia

Abstract

The mechanism of methane dissociation on an Rh-decorated Ni(100) surface has been investigated Using density functional theory. The study includes the determination of the most stable adsorbate/adsorbent configurations of the species associated with subsequent reactions and generating the energy surface for CH_4 dissociation process. The Rh-decorated Ni(100) surface was found to be more favorable for the process than the NiRh(111) configuration, mainly due to lower the activation energy of CH decomposition reaction by 48.5%, leading to a higher conversion of CH_4 to carbon and hydrogen

Paper type: Research paper

Keywords: DFT; methane; dehydrogenation; cracking

Citation: Ibrahim Suleiman, Niveen Assaf, Michael Stockenhuber, and Eric M Kennedy "Methane dissociation over the Rh-Decorated Ni(100) Surface: A density functional theory investigation" *Jordanian Journal of Engineering and Chemical Industries*, Vol. **4**, No.2, pp:38-43 (2021).

Introduction

The production of hydrogen and carbon via the catalytic cracking of methane has attracted the attention of many researchers (Abbas and Daud, 2010; Abbas and Wan Daud, 2010; Amin *et al.*, 2012; Amin *et al.*, 2011; Ashik *et al.*, 2017; Fan *et al.*, 2012; He *et al.*, 2018; Italiano *et al.*, 2010; Li *et al.*, 2018; Serrano *et al.*, 2010; Tezel *et al.*, 2019; Zhang *et al.*, 2017; Zou *et al.*, 2019). Methane is hydrogen-rich with a lower carbon supply rate, which can reduce the process of graphene growth on the catalyst (Yang and Chen, 1989; Zhu *et al.*, 2007). Transition metals, notably, Ni-based catalysts have shown high efficiency for methane dehydrogenation reaction (Amin *et al.*, 2012; Fan *et al.*, 2012; He *et al.*, 2015; Li *et al.*, 2015b; Liu *et al.*, 2011; Shadravan *et al.*, 2018; Wang *et al.*, 2006; Zhu *et al.*, 2007). The mechanism of CH_4 dissociation has been investigated both experimentally and theoretically. Using high-resolution electron energy loss spectroscopy (HREELS) (Lee *et al.*, 1987; Lee *et al.*, 1985) and X-ray photoelectron spectroscopy (XPS) techniques (Kaminsky *et al.*, 1986; Yang *et al.*, 1995), chemisorbed CH_3, CH_2, and CH species have been observed on the Ni surface indicating that CH_4 is transforming into C and H_2 through sequential $CH_{(x:4-1)}$ dehydrogenation reactions. The mechanism of methane cracking appears to have the following steps:

$$CH_{4(g)} + 2 * \rightleftharpoons CH_{3(ads)} + H_{(ads)} \quad (1)$$

$$CH_{3(ads)} + * \rightleftharpoons CH_{2(ads)} + H_{(ads)} \quad (2)$$

$$CH_{2(ads)} + * \rightleftharpoons CH_{(ads)} + H_{(ads)} \quad (3)$$

$$CH_{(ads)} + * \rightleftharpoons C_{(ads)} + H_{(ads)} \quad (4)$$

where the asterisk (*) denotes an active site on the surface, and (ads) means adsorbed species on the surface (Li *et al.*, 2015b).

* Corresponding author: E-mail: dr.ibrahim.suleiman@bau.edu.jo dr.ibrahim.suleiman@gmail.com ORCID: https://orcid.org/0000-0002-7311-9227
Received on May 26, 2021; Accepted on July11, 2021.
Jordanian Journal of Engineering and Chemical Industries (JJECI), Vol.4, No.2, 2021, pp. 38-43.

Bimetallic Ni-based catalysts were recently used to improve catalyst stability and activity. Various studies have shown that bimetallic Ni-based catalysts are more durable and lead to higher CH_4 conversion levels (Fan *et al.*, 2012; He *et al.*, 2015; He *et al.*, 2018; Horváth *et al.*, 2011; Jia *et al.*, 2020; Li *et al.*, 2013; Liu *et al.*, 2011; Tezel *et al.*, 2019; Theofanidis *et al.*, 2020; Tian *et al.*, 2018). Rhodium is known as a suitable catalyst for the hydrogen evolution reaction (HER). However, due to its high cost, many studies have been carried out to develop a catalyst characterized by high performance with low Rh content (Huang *et al.*, 2017; Nguyen and Choi, 2019; Nguyen *et al.*, 2019). Li *et al* (Li *et al.*, 2013) have studied the dissociation of CH_4 on the NiRh(111) surface and compared it with various bimetallic Ni-based catalysts using DFT calculations. They have reported that NiRh have higher catalytic activity for CH_4 dissociation than other catalysts. The effect of the orientation of the catalyst surface on methane decomposition was investigated. Yang and Chen have shown that the Ni(100) and Ni(110) are among the gas/metal interface, whereas Ni(111) and Ni(311) belong to the graphite/metal interface. In their study, they concluded that the activation energy required for CH_4 dissociation on Ni(100) was lower than that on Ni(111) (Zhu *et al.*, 2007). In this study the (100) orientation is incorporated with doping Rh with Ni to investigate the mechanism of CH_4 cracking process. The aim is to show that the Rh-Ni(100) surface is more adroit for the abovementioned process compared to the NiRh(111) configuration, particularly, for the CH dissociation step.

1 Materials and Methods

1.1 Computational Method

Density functional theory calculations were carried out to investigate the mechanism of CH_4 dissociation on the Rh-Ni(100) surface using DMol^3 code (Delley, 1990; 2000). The generalized gradient approximation of Perdew and Wang (GGA-PW91) (Perdew and Burke, 1996; Perdew *et al.*, 1996) was used in this study in conjunction with a double numeric quality basis set with polarization functions (DNP). The smearing parameter and space cutoff was set to be 0.14 eV and 4.6 Å, respectively. Adopting the models of Fan *et al.* (Fan *et al.*, 2012), Li *et al.* (Li *et al.*, 2014), and Li *et al.* (Li *et al.*, 2013), asymmetric four-layer slabs, separated by a vacuum of 10 Å, were used in all calculations. However, the binding energies of CH, CH_2 and H were tested using 4-layer slab fixing the bottom two layers and four-layer slab fixing the most bottom layer. The results were similar, where the binding energies using the latter model were found to be larger at most by 2.08 kcal/mol. Therefore, the total energies of the slabs were minimized by allowing the top two layers of the slab and the adsorbates to move. The tolerances on the energy, gradient and displacement convergence were set to 2.7×10^{-5} eV, 5.4×10^{-4}eV/Å, and 5×10^{-3} Å, respectively. The dipole slab correction was applied to neutralize the dipole moment resulting from using asymmetric slabs. A (3×3) unit cells, with a $3 \times 3 \times 1$ Monkhorst–Pack (Monkhorst and Pack, 1976) k-point sampling set were used to investigate the reactions and the adsorption of different species associated with them. Transition state structure searches were conducted using the Linear (LST) and Quadratic (QST) synchronous transit methods.

2 Results and Discussion

2.1 The isolated CH_4 molecule and clean Rh-Ni(100) surface

The C-H bond length and the H-C-H angle of an isolated CH_4 molecule were calculated to be 1.099 Å and 109.471°, respectively. The calculated C-H bond length was more significant than the experimental value of 1.087 Å (Hirota, 1979) by 1.1 %. The estimated H-C-H angle is less than the experimental value of 109.5° (Van Vleck, 1934) by 0.02%. The Rh-Ni(100) surface was modeled by replacing only one Ni atom of the most top layer in the unit cell with an Rh atom, as shown in **Figure 1**. The Rh atom was prominent compared to Ni atoms in the topmost layer by 0.16 Å, as illustrated in Figure 1 (B). The average distance between the first and second layers of the slab, d_{12}. was found to be 1.74 Å [See Fig. 1 (B)], showing an inward relaxation of 2.7% compared to the bulk distance. The pure Ni(100) surface also shows, using DFT calculations, an inward relaxation of 7.7% (Zhu *et al.*, 2007). Therefore, the presence of Rh atom inhibits surface relaxation; however, this could enhance the process of carbon diffusion into the slab, resulting in the formation and growth of graphene or carbon nano-tubes (Li *et al.*, 2015a, b).

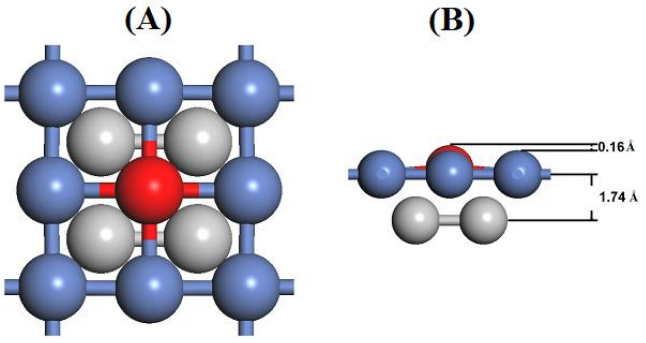

Fig.1 (A) Top and (B) side views of a (3×3) unit cell of an Rh-decorated Ni(100) surface. Blue and grey balls represent Ni atoms in the first and second layers, respectively. The red ball represents the Rh atom.

Six sites are available on the surface for the adsorption of CH_x species as well as carbon and hydrogen, as shown in **Figure 2**. The binding energies between the adsorbates and the adsorbent were calculated using the equation:

$$E_b = \frac{1}{n}\left[E_{x/slab} - E_{slab} - nE_x\right] \quad (5)$$

where E_{slab}, E_x, and $E_{x/slab}$ are the total energies of a clean slab, an isolated x atom/molecule, and the x/slab adsorption system, respectively, with n being the number of adsorbed species within each supercell. The most stable configurations for the chemical species on the surface are listed in **Table 1** and their binding energies. To determine the reaction energetics, as well as transition states, the most stable adsorption configurations for various species associated with the CH_4 dissociation reactions on the surface have been used.

Site	Notation
Bridge between Rh and Ni atoms	B_Rh
Bridge between two Ni atoms	B_Ni
Top on Rh atom	T_Rh
Top on Ni atom next to Rh atom	T_Ni1
Top on Ni atom far from Rh atom	T_Ni2
Hollow	Hollow

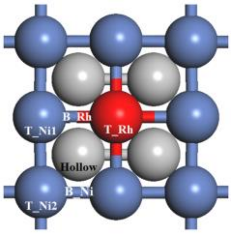

Fig. 2 Schematic diagram of a top view of the surface showing the different possible adsorption sites on it. Blue and grey balls represent Ni atoms in the first and second layers, respectively. The red ball represents the Rh atom.

2.2 CH_4 adsorption and dissociation

The following reactions can describe methane adsorption and dissociation

$$CH_{4(g)} + * \rightleftharpoons CH_{4(ads)} \quad (R1)$$

$$CH_{4(ads)} + * \rightleftharpoons CH_{3(ads)} + H_{(ads)} \quad (R2)$$

It was found that methane is weakly adsorbed on the surface, where the most stable site is B_Rh (see Fig. 2) with a binding energy of -7.39 kcal/mol; inconsistent with the results of Li *et al.*(Li *et al.*, 2013) (-6.93 kcal/mol) and Zhu *et al.*(Zhu *et al.*, 2007) (-2.08 kcal/mol) for CH_4 adsorption on NiRh(111) and Ni(100), respectively. Reaction (R2) was found to be endothermic by -.32 kcal/mol and with a transition state barrier of 21.60 kcal/mol. The reactants, transition state, and products configurations are shown in **Figure 3**. Using NiRh(111), Li et al (Li *et al.*, 2013), and Fan *et al.* (Fan *et al.*, 2012)found that this reaction is endothermic with a barrier of 17.32 kcal/mol and 17.79 kcal/mol, respectively. These results indicate that the NiRh(111) surface is more favorable for CH_4 dissociation.

Table 1: Most stable adsorption sites for the chemical species on the Rh-Ni (100) surface and their binding energies in kcal/mol

Species	Most Stable site	Binding Energy
C	Hollow	-186.19
H	Hollow	-65.84
CH	Hollow	-161.70
CH_2	Hollow	-100.49
CH_3	B_Ni	-47.82
CH_4	B_Rh	-7.39

2.3 CH_3 adsorption and dissociation

The most stable sites for CH_3 adsorption was predicted to be B_Ni followed by B_Rh (see Fig 2) with binding energies of -47.82 and 46.66 kcal/mol, respectively. The binding energies were calculated to be -45.74 and -42.04 kcal/mol for CH_3 on the Ni(100) and NiRh(111) surfaces, respectively.

The dissociation of CH_3 is described by the reaction

$$CH_{3(ads)} + * \rightleftharpoons CH_{2(ads)} + H_{(ads)} \quad (R3)$$

The reaction was found to be endothermic by 0.76 kcal/mol and has a barrier of 15.5 kcal/mol. The reactants, transition state, and products configurations are shown in **Figure 4**. The reaction was reported to be exothermic on the NiRh(111) surface with a critical barrier of 9.93 kcal/mol (Li *et al.*, 2013). Fan. (Fan *et al.*, 2012) found that reaction slightly endothermic with a 13.17 kcal /mol barrier energy. This gives the advantage for the NiRh(111) surface for this reaction.

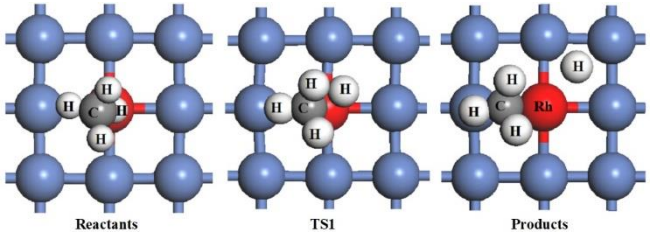

Fig. 3 Initial, transition state and final configurations associated to reaction R2. Blue large balls represent Ni atoms, the large red ball represents Rh atom, the smaller grey ball represents C atom, and white balls represent H atoms.

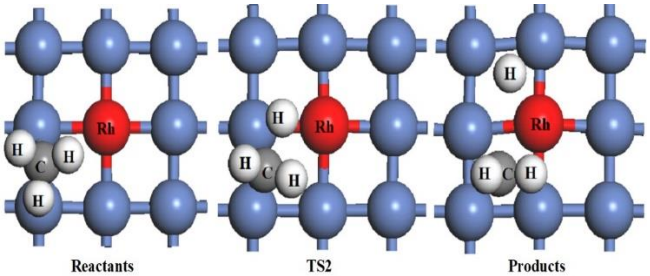

Fig. 4 Initial, transition state and final configurations associated to reaction R3.

2.4 CH_2 adsorption and dissociation

The hollow site was found to be the most stable for CH_2 adsorption with a binding energy of -100.49 kcal/mol. The dissociation reaction of CH_2 is described by the equation:

$$CH_{2(ads)} + * \rightleftharpoons CH_{(ads)} + H_{(ads)} \quad (R4)$$

The reaction was exothermic on the Rh-Ni(100) surface by 14.1 kcal/mol and has a 5.96 kcal/mol barrier. The reactants, transition state, and products configurations are shown in **Figure 5**. Fan (Fan *et al.*, 2012) reported that this reaction exhibits an exothermic nature with an activation energy of 5.78 kcal/mol. Li *et al.* (Li *et al.*, 2013) have reported this reaction to be exothermic by 5.47 kcal/mol on NiRh(111), however, with a lower barrier of 3.28 kcal/mol, which gives the advantage to the (111) configuration for CH_2 dissociation.

2. 5 CH adsorption and dissociation

The hollow site was the most stable site for CH adsorption, with a binding energy of -161.70 kcal/mol. The CH dissociation takes place according to the reaction

$$CH_{(ads)} + * \rightleftharpoons C_{(ads)} + H_{(ads)} \quad \text{(R5)}$$

The calculations show that this reaction has an exothermicity of 1.22 kcal/mol and requires a barrier of 16.8 kcal/mol. The reactants, transition state, and products configurations are shown in **Figure 6**. Reaction (R5) was stated to be endothermic on NiRh(111) by 15.25 kcal/mol and requires a barrier of 29.8 kcal/mol (Li *et al.*, 2013). Fan (Fan *et al.*, 2012) have also found that this reaction is endothermic and requires a 32.11 kcal/mol activation energy. These results show that the Rh-Ni(100) surface is more adroit for the CH dissociation reaction. Atomic carbon and hydrogen were found to be adsorbed on the hollow site with binding energies of -186.19 and -65.84 kcal/mol, respectively.

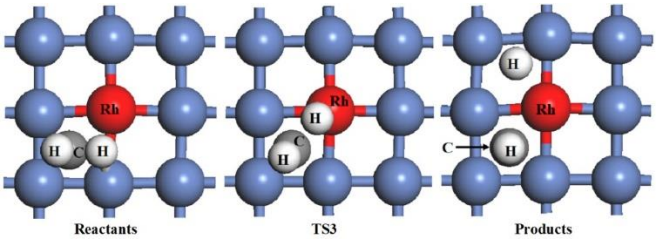

Fig. 5 Initial, transition state and final configurations associated to reaction R4.

2.6 The overall reaction

Figure 7 shows the energies along with the coordinates of the overall reaction $CH_{4(g)} \rightleftharpoons C_{(ads)} + 4H_{(ads)}$ over the Rh-Ni(100) and NiRH(111) surfaces. **Figure 7** gives a better understanding of the whole process and explains which surface best facilitates the whole CH_4 dissociation process.

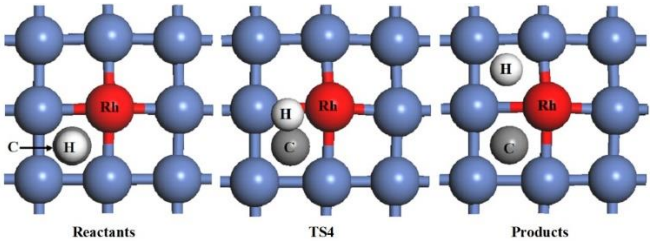

Fig. 6 Initial, transition state and final configurations associated to reaction R5.

From the discussion above, the NiRh(111) surface was found to be more favorable for the reactions (R2), (R3), and (R4), whereas Rh-Ni(100) was found more preferable for reaction (R5) for the lower required barriers. This is true if these reactions were carried out individually, but the reactions simultaneously occur on the surface. The complete process, therefore, should be taken into account, and here, two particular processes will be discussed; these are CH_3 and CH dissociation reactions. The dissociation of CH_3 can be described by the equation $CH_4 \xleftarrow{E_{a_{-R2}}} CH_3 + H \xrightarrow{E_{a_{R3}}} CH_2 + 2H$, where $E_{a_{R3}}$ is the activation energy of the forward reaction of R3 and $E_{a_{-R2}}$ is the activation energy of the backward reaction of R2. On the NiRh(111) surface, $E_{a_{R3}}$ was found to be 9.93 kcal/mol (Li *et al.*, 2013), lower than the activation energy required for the same reaction on the Rh-Ni(100) surface by 5.57 kcal/mol. However, $E_{a_{-R2}}$ for the reformation of CH_4 was found to be 9.70 kcal/mol using NiRh(111), which is lower than the barrier needed for CH_3 dissociation by 0.23 kcal/mol. This means that if there is a hydrogen atom next to the CH_3 entity on the NiRh(111) surface, the reformation of CH_4 will be more likely to occur. On the other hand, the barrier of CH_4 reformation reaction on the Rh-Ni(100) surface is calculated to be 17.28 kcal/mol, which is higher than the barrier of CH_3 dissociation by 1.78 kcal/mol, giving the advantage to the reaction to go further towards CH_2 and H production. Thus, the Rh-Ni(100) surface is anticipated to be better for this reaction than NiRh(111), notably, if an atomic hydrogen coexists with CH_3 on the surface. The dissociation of CH was reported to be a limiting step for CH_4 decomposition reaction on NiRh(111) due to the required activation energy (Li *et al.*, 2013; Zhu *et al.*, 2007). The

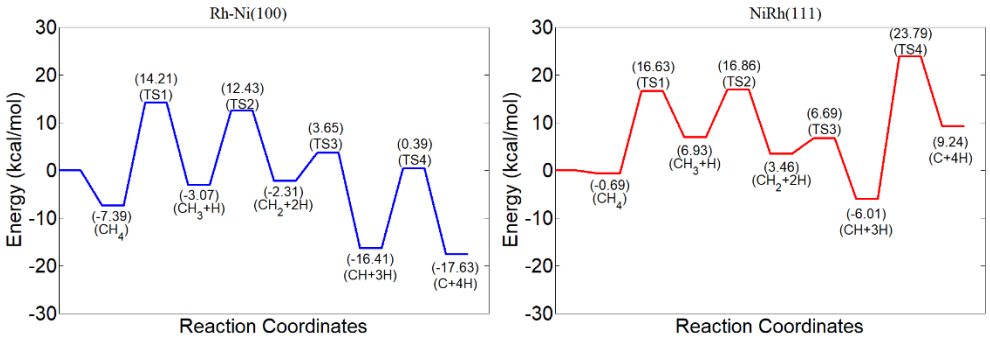

Fig. 7 The potential energy surfaces for CH_4 dissociation on Rh-Ni(100) and NiRh(111) surfaces.

process of CH decomposition can be described by: $CH_2 \xleftarrow{E_{a_{-R4}}} CH + H \xrightarrow{E_{a_{R5}}} C + 2H$ where $E_{a_{R5}}$ is the activation energy of the forward reaction of R5 and $E_{a_{-R4}}$ is the activation energy of the backward reaction of R4.

The value of $E_{a_{R5}}$ was calculated to be 16.80 kcal/mol and 29.78 kcal/mol using the Rh-Ni(100) and NiRh(111) surface, respectively, giving the advantage for the Rh-Ni(100) surface. Besides, the dissociation of CH on NiRh(111) requires a barrier of 29.8 kcal/mol, whereas the barrier of the backward reaction of $CH_{2(ads)} + * \rightleftharpoons CH_{(ads)} + H_{(ads)}$ needs a barrier of 12.70 kcal/mol (Li *et al.*, 2013), which means that if atomic hydrogen coexists next to an adsorbed CH entity, the reformation of CH_2 is more likely to take place instead of CH splitting. Using Rh-Ni(100), the barrier of CH dissociation is lower than the activation energy required for CH_2 reformation by 16.3%, giving the benefit to the reaction to go further towards C and H formation, leading therefore, to a higher conversion of CH to C and H.

Conclusions

The mechanism of the reaction $CH_{4(g)} \rightleftharpoons C_{(ads)} + 4H_{(ads)}$ was investigated using DFT calculations for the periodic slab on the Rh-Ni(100) surface. It was shown that methane is weakly adsorbed on the surface and requires a 21.60 kcal/mol barrier to dissociate. The results of this investigation were compared to the results of the same reaction over NiRh(111). It was shown that the NiRh(111) configuration is more favorable for reactions R2, R3, and R4 if each reaction was carried out individually on the surface, whereas Rh-Ni(100) is better for the reaction R5. However, the Rh-Ni(100) surface was found to benefit the complete process in a better way, due to the decrease in the energy level of barriers along with the reaction coordinates, which leads to a higher conversion of CH_4 to carbon and hydrogen.

Acknowledgment

This research was undertaken on the NCI national facility in Canberra, Australia, supported by the Australian Commonwealth Government. Intersect Australia Ltd also provided computational resources used in this work.

Nomenclature

E_{a_-}	=the activation energy of the backward reaction	[kcal/mol]
E_{a}	=the activation energy of the forward reaction	[kcal/mol]
E_{slab}	=total energy of a clean slab	[kcal/mol]
E_x	=total energy of isolated x atom/molecule	[kcal/mol]
$E_{x/slab}$	=total energy of the x/slab adsorption system	[kcal/mol]
n	=the number of adsorbed species within each supercell	[atom or molecule]

References

Abbas, H. F., and W., Daud "Hydrogen production by thermocatalytic decomposition of methane using a fixed bed activated carbon in a pilot scale unit: Apparent kinetic, deactivation and diffusional limitation studies", *Int. J of Hydrogen Energy*, **35**, 12268-12276 (2010).

Abbas, H. F., and W., Daud, "Hydrogen production by methane decomposition: A review", *Int. J. of Hydrogen Energy*, **35**, 1160-1190 (2010).

Amin, A. M., Croiset, E., Constantinou, C., and W., Epling "Methane cracking using Ni supported on porous and non-porous alumina catalysts", *Int. J. of Hydrogen Energy*, **37**, 9038-9048 (2012).

Amin, A. M., Croiset, E., and W., Epling "Review of methane catalytic cracking for hydrogen production", *Int. J. of Hydrogen Energy*, **36**, 2904-2935 (2011).

Ashik, U. P. M., Wan Daud, W. M. A., and J., Hayashi "A review on methane transformation to hydrogen and nanocarbon: Relevance of catalyst characteristics and experimental parameters on yield", *Renewable. and Sust. Energy Rev.*, **76**, 743-767 (2017).

Delley, B. "An all-electron numerical method for solving the local density functional for polyatomic molecules", *The J. of Chem. Phy.*, **92**, 508-517 (1990).

Delley, B. "From molecules to solids with the DMol3 approach", *J. of Chem. Physics*, **113**, 7756-7764 (2000).

Fan, C., Zhu, Y. A., Xu, Y., Zhou, Y., Zhou, X. G., and D., Chen "Origin of synergistic effect over Ni-based bimetallic surfaces: A density functional theory study", *The J. of Chem. Physics*, **137**, 014703 (2012).

He, F., Li, K., Xie, G., Wang, Y., Jiao, M., Tang, H., and Z., Wu "Theoretical insights on the influence of doped Ni in the early stage of graphene growth during the CH_4 dissociation on Ni–Cu(111) surface", *Appl. Catalysis A:General*, **506**, 1-7 (2015).

He, J., Yang, Z., Ding, C., Zhang, L., Yan, Y., and X., Du "Methane dehydrogenation and oxidation process over Ni-based bimetallic catalysts", *Fuel* **226**, 400-409 (2018).

Hirota, E. "Anharmonic potential function and equilibrium structure of methane", *J. of Molec. Spect.*, **77**, 213-221 (1979).

Horváth, A., Stefler, G., Geszti, O., Kienneman, A., Pietraszek, A., and L., Guczi "Methane dry reforming with CO_2 on CeZr-oxide supported Ni, NiRh and NiCo catalysts prepared by sol–gel technique: Relationship between activity and coke formation", *Catalysis Today*, **169**, 102-111 (2011).

Huang, L., Jiao, C., Wang, L., Huang, Z., Liang, F., Liu, S., Wang, Y., Zhang, H., and S., Zhang "Preparation of Rh/Ag bimetallic nanoparticles as effective catalyst for hydrogen generation from hydrolysis of KBH_4", *Nanotechnology*. **29**, 044002 (2017).

Italiano, G., Delia, A., Espro, C., Bonura, G., and F., Frusteri "Methane decomposition over Co thin layer supported catalysts to produce hydrogen for fuel cell". *Int. J.l of Hydrogen Energy*, **35**, 11568-11575 (2010).

Jia, J., Veksha, A., Lim, T. T., and G., Lisak "In situ grown metallic nickel from X–Ni (X=La, Mg, Sr) oxides for converting plastics into carbon nanotubes: Influence of metal–support interaction", *J. of Cleaner Prod.*, **258** (2020).

Kaminsky, M. P., Winograd, N., Geoffroy, G. L., and M., Vannice "Direct SIMS Observation of Methylidyne, Methylene, and Methyl Intermediates on a Ni(111) Methanation Catalyst", *J. of the Amer. Chem. Soc.*, **108**, 1315-1316 (1986).

Lee, M. B., Yang, Q. Y., and S., Ceyer "Dynamics of the activated dissociative chemisorption of CH_4 and implication for the pressure gap in catalysis: A molecular beam-high resolution electron energy loss study", *The J. of Chem. Phy.*, **87**, 2724-2741 (1987).

Lee, M. B., Yang, Q. Y., Tang, and S., Ceyer "Activated dissociative chemisorption of CH_4 on Ni(111): Observation of a methyl radical and implication for the pressure gap in catalysis", *The J. of Chem. Phy.*, **85**, 1693-1694 (1985).

Li, J., Croiset, E., and L., Ricardez-Sandoval "Carbon nanotube growth: First-principles-based kinetic Monte Carlo model", *J. of Catalysis* **326**, 15-25 (2015a).

Li, J., Croiset, E., and L., Ricardez-Sandoval "Theoretical investigation of the methane cracking reaction pathways on Ni (111) surface", *Chem. Phy. Letters*, **639**, 205-210 (2015b).

Li, J., Croiset, E., and L., Ricardez–Sandoval "Effect of carbon on the Ni catalyzed methane cracking reaction: A DFT study", *App. Surf. Sci.*, **311**, 435-442 (2014).

Li, K., Jiao, M., Wang, Y., and Z., Wu "CH_4 dissociation on NiM(111) (M=Co, Rh, Ir) surface: A first-principles study", *Surf. Sci.*, **617**, 149-155 (2013).

Li, K., Li, H., Yan, N., Wang, T., and Z., Zhao "Adsorption and dissociation of CH_4 on graphene: A density functional theory study", *App. Sur. Sci.*, **459**, 693-699 (2018).

Liu, H., Yan, R., Zhang, R., Wang, B., and K., Xie "A DFT theoretical study of CH_4 dissociation on gold-alloyed Ni(111) surface", *J. of Nat. Gas Chem.*, **20**, 611-617 (2011).

Monkhorst, H. J., and J., Pack "Special points for Brillouin-zone integrations", *Phy.l Rev., B* **13**, 5188-5192 (1976).

Nguyen, N.-A., and H., Choi "Effect of Ni/Rh ratios on characteristics of NixRhy nanosponges towards high-performance hydrogen evolution reaction", *Data in Brief*, **24**, 103941 (2019).

Nguyen, N. A., Nguyen, V. T., Shin, S., and H., Choi "NiRh nanosponges with highly efficient electrocatalytic performance for hydrogen evolution reaction", *J. of Alloys and Comp.*, **789**, 163-173 (2019).

Perdew, J. P., and K., Burke "Generalized gradient approximation for the exchange-correlation hole of a many-electron system", *Phy. Rev. B - Condensed Matter and Mat Phy.*, **54**, 16533-16539 (1996).

Perdew, J. P., Burke, K., and M., Ernzerhof "Generalized gradient approximation made simple". *Physical Review Letters* **77**, 3865-3868 (1996).

Serrano, D. P., Botas, J. A., Fierro, J. L. G., Guil-López, R., Pizarro, P., and G., Gómez "Hydrogen production by methane decomposition: Origin of the catalytic activity of carbon materials", *Fuel*, **89**, 1241-1248 (2010).

Shadravan, V., Kennedy, E., and M., Stockenhuber "An experimental investigation on the effects of adding a transition metal to Ni/Al_2O_3 for catalytic hydrogenation of CO and CO_2 in presence of light alkanes and alkenes", *Catalysis Today*, **307**, 277-285 (2018).

Tezel, E., Figen, H.E., and S., Baykara "Hydrogen production by methane decomposition using bimetallic Ni–Fe catalysts", *Int. J. of Hydrogen Energy*, **44**, 9930-9940 (2019).

Theofanidis, S. A., Pieterse, J. A. Z., Poelman, H., Longo, A., Sabbe, M. K., Virginie, M., Detavernier, C., Marin, G. B., and V., Galvita "Effect of Rh in Ni-based catalysts on sulfur impurities during methane reforming", *App. Catalysis B: Env.*, **267**, 118691 (2020).

Tian, B., Liu, T., Yang, Y., Li, K., Wu, Z., and Y., Wang "CH_4 dissociation in the early stage of graphene growth on Fe–Cu(100) surface: Theoretical insights", *App.Sur. Sci.*, **427**, 953-960 (2018).

Van Vleck, J. H. "On the Theory of the Structure of CH_4 and Related Molecules: Part III" *The J. of Chem. Phy.*, **2**, 20-30 (1934).

Wang, S. G., Cao, D. B., Li, Y. W., Wang, J., and H., Jiao "CH_4 dissociation on Ni surfaces: Density functional theory study", *Sur. Sci.*, **600**, 3226-3234 (2006).

Yang, Q. Y., Maynard, K. J., Johnson, A. D., and S. Ceyer "The structure and chemistry of CH_3 and CH radicals adsorbed on Ni(111)", *The J. of Chem. Phy.*, **102**, 7734-7749 (1995).

Yang, R. T., and J., Chen "Mechanism of carbon filament growth on metal catalysts", *J. of Catalysis*, **115**, 52-64 (1989).

Zhang, J., Li, X., Chen, H., Qi, M., Zhang, G., Hu, H., and X., Ma "Hydrogen production by catalytic methane decomposition: Carbon materials as catalysts or catalyst supports", *Int. J. of Hydrogen Energy*, **42**, 19755-19775 (2017).

Zhu, Y. A., Dai, Y. C., Chen, D., and W. Yuan "First-principles calculations of CH_4 dissociation on Ni(100) surface along different reaction pathways", *J. of Mol. Catalysis A: Chem.*, **264**, 299-308 (2007).

Zou, J., Rezaee, R., Xie, Q., and L., You "Characterization of the combined effect of high temperature and moisture on methane adsorption in shale gas reservoirs", *J. of Pet.Sci. and Eng.*, **182**, 106353 (2019).